






Molecular Landscape of Endometrial Stromal Tumors

Marta Brunetti, PhD¹ ; Valeria Vitelli, PhD² ; Anca Mihaela Naas, MD³; Ane Gerda Zahl Eriksson, MD, PhD⁴; Hans Kristian Haugland, MD, PhD⁵ ; Camilla Krakstad, PhD^{6,7} ; and Francesca Micci, PhD¹ 

DOI <https://doi.org/10.1200/PO-24-00779>

ABSTRACT

PURPOSE The molecular heterogeneity of endometrial stromal tumors (ESTs) is demonstrated by the presence of the same fusion gene in distinct pathologic entities, such as endometrial nodules and low-grade endometrial stromal sarcoma, both exhibiting the *JAZF1::SUZ12* chimeric transcript. Given the limited knowledge on these tumors, which is based on a small number of cases studied with a restricted range of techniques, we analyzed 47 ESTs to explore their methylation and transcriptomic landscapes.

MATERIALS AND METHODS Tumor methylation and transcriptomes profiles were investigated.

RESULTS The methylation profile showed distinct clusters, which correlated with established histopathologic and molecular subtypes. The highest methylation value was reported for nuclear factor of activated T cytoplasmic 1, and the lowest was detected for *miR34C*. Two different 5'—C—phosphate—G—3' (CpG) sites of *LMX1B* (*LMX1B-cg04996334* and *LMX1B*), along with *miR34C*, showed the same methylation pattern in both low-grade and high-grade endometrial stromal sarcoma (HG-ESS). Similarly, *CFAP45*, *HDAC4*, *ACY3*, *MOB3A*, and *XXYL1* showed identical methylation patterns in HG-ESS and undifferentiated uterine sarcomas, highlighting the similarities between these tumors within the EST spectrum. We identified 13 novel fusion transcripts involving several genes that are active in transcriptional regulation.

CONCLUSION In ESTs, the genes involved in chromosomal rearrangements function as transcription regulators, either directly through the formation of zinc finger motifs or indirectly through epigenetic regulation. The methylation signature is different for distinct subgroups of the EST spectrum, with more aggressive tumors, HG-ESS, and undifferentiated uterine sarcoma, clustering together. Some genes showed similar methylation levels in different entities, highlighting the presence of a continuum in the tumor profile. Methylation levels of CpG sites at specific gene loci may serve as valuable biomarkers for these tumors.

ACCOMPANYING CONTENT

 Appendix

Accepted March 19, 2025

Published May 22, 2025

JCO Precis Oncol 9:e2400779

© 2025 by American Society of Clinical Oncology

Creative Commons Attribution
Non-Commercial No Derivatives
4.0 License

INTRODUCTION

Endometrial stromal tumors (ESTs) are a rare and heterogeneous group of mesenchymal tumors originating from the smooth muscle of both the myometrium and endometrial stroma,¹ representing approximately 10% of uterine mesenchymal tumors.² The WHO (2020)¹ has divided ESTs into four subgroups: (1) endometrial stromal nodules (ESNs), (2) low-grade endometrial stromal sarcomas (LG-ESSs), (3) high-grade endometrial stromal sarcomas (HG-ESSs), and (4) undifferentiated uterine sarcomas (UUSs). The spectrum ranges from benign tumors, characterized by well-circumscribed margins and cells resembling proliferative-phase endometrial stroma, to low-grade malignant and

malignant tumors, which display invasive growth into the surrounding myometrium, and finally to highly aggressive tumors, marked by high-grade cytologic features without specific differentiation.³ Although the genetic signature of ESS is characterized by the presence of chromosomal aberrations leading to gene fusions,^{3,4} ESN and UUS do not show any specific genomic alterations.⁴ The cytogenetic hallmark of LG-ESS is the 7;17-chromosomal translocation, leading to the fusion *JAZF1::SUZ12*,⁵ followed in frequency by rearrangements of chromosome band 6p21 leading to *PHF1* fusion⁶; the *YHWA::NUMT2A/B* and *ZC3H7B::BCOR* fusions seem to be specific for HG-ESS.^{4,7} Some entities show the morphologic characteristics of a specific subgroup but possess molecular features typical of another. For example, the *JAZF1::SUZ12*

CONTEXT

Key Objective

We report the molecular landscape of endometrial stromal tumors (ESTs). Given the rarity of these tumors, this is the largest cohort analyzed so far.

Knowledge Generated

We explored EST methylation and transcriptomic landscapes. The methylation profile showed distinct clusters, which correlated with established histopathologic and molecular subtypes. The methylation signature differed for distinct EST spectrum subgroups, with more aggressive tumors, high-grade endometrial stromal sarcoma, and undifferentiated uterine sarcoma, clustering together. Some genes showed similar methylation levels in different entities, highlighting the presence of a continuum in the tumor profile. Thirteen novel fusion transcripts involving several genes that are active in transcriptional regulation were identified.

Relevance

Methylation levels of CpG sites at specific gene loci may serve as valuable biomarkers for these tumors. The presence of specific fusion genes is a characteristic of the EST subtype.

fusion and *PHF1* rearrangements have also been identified in a few ESNs.^{8–10} Moreover, some ESSs do not display any known fusion transcripts at the molecular level, making their diagnosis challenging.^{11,12} This suggests the presence of additional, yet unidentified, mechanisms underlying tumorigenesis and progression. Consequently, we screened 47 ESTs to build a detailed molecular landscape from both DNA and RNA data to overcome the knowledge gap in these tumors.

MATERIALS AND METHODS

Tumor Material

The study included 47 ESTs, of which 24 were LG-ESSs, nine HG-ESSs, five UUSs, two ESNs, and seven ESSs with undefined grades (Table 1). All tumors were reviewed and the diagnoses based on the 2020 WHO criteria. Twenty-eight tumors were surgically excised at the Norwegian Radium Hospital (Oslo, Norway), as previously reported,^{3,6,7} whereas 19 were obtained from Haukeland University Hospital (Bergen, Norway). The study was approved by the Regional Committee for Medical and Health Research Ethics (REK; 2.2007.425 and 2011-2071), and the protocol was approved by the institutional review board at Oslo universitetssykehus HF. The Ethics Committee has approved the use of the patient material under the provision of consent from each living patient.

DNA and RNA Extraction

Fresh frozen material from a representative area of all tumors was used to extract DNA and RNA. DNA was extracted using the Maxwell 16 extractor (Promega, Madison, WI)^{14,15} and then purified using the Maxwell 16 Cell DNA Purification kit (Promega), Maxwell RSC DNA Formalin-Fixed Paraffin-Embedded (FFPE) Kit (Promega), and AllPrep DNA/RNA Mini Kit (Qiagen, Hilden, Germany) according to the

manufacturer's recommendations. RNA was extracted using the miRNeasy kit and AllPrep DNA/RNA Mini Kit (Qiagen). In six cases, material FFPE blocks were used to extract DNA using the Maxwell RSC DNA FFPE Kit (Promega). Concentrations were measured using a QIAxcel microfluidic ultraviolet visible spectrophotometer (Qiagen, Hilden, Germany) and a Quantus fluorometer (Promega). RNA quality was assessed with an Agilent RNA 6000 Nano Total Kit on an Agilent 2100 Bioanalyzer (Agilent Technologies, Germany).

Array-Based DNA Methylation Profiling

Thirty-eight tumors with available material (24 LG-ESSs, nine HG-ESSs, and five USSs) were analyzed using the Illumina Infinium Human Methylation 450 (450k) or EPIC (850k) BeadChip (Illumina, San Diego, CA), according to the manufacturer's instructions, at the Genomics Core Facility, Oslo University Hospital, Oslo, Norway.¹⁶ Raw DNA methylation data were imported, preprocessed, and normalized with the minfi R package^{17,18} (version 1.46.0). All subsequent analyses were performed using R software for statistical computing (version 4.3.1).¹⁹ Preprocessing included channel matching (using the function "preprocessIllumina"), dropping the probes containing a single nucleotide polymorphism at the CpG interrogation or at the single nucleotide extension (using the function "dropLociWithSnps"), removing the probes targeting sex chromosomes and those which included missing values for any of the samples. DNA methylation data were normalized using background subtraction and control normalization.

Clustering and Statistical Analysis

Principal component analysis (PCA)²⁰ was performed on the scaled data to capture variability patterns and reduce dimensionality. Only principal components leading to a

TABLE 1. Diagnosis and fusion Transcripts Identified in 47 Endometrial Stromal Tumors

Patient	Diagnosis	Fusion Transcripts
1 ^a	LG-ESS	
2 ^a	LG-ESS	JAZF1::SUZ12
3 ^a	LG-ESS	JAZF1::SUZ12
4 ^a	LG-ESS	
5 ^a	LG-ESS	
6 ^a	LG-ESS	MEAF6::PHF1
7 ^a	HG-ESS	ZC3H7B::BCOR
8 ^a	LG-ESS	
9 ^a	LG-ESS	
10 ^a	LG-ESS	JAZF1::PHF1
11 ^a	LG-ESS	JAZF1::SUZ12
12	NOS	
13 ^a	LG-ESS	JAZF1::PHF1
14 ^a	LG-ESS	MEAF6::PHF1
15 ^a	LG-ESS	JAZF1::SUZ12
16 ^a	LG-ESS	EPC1::PHF1
17	LG-ESS	JAZF1::PHF1
18	LG-ESS	JAZF1::SUZ12
19 ^a	LG-ESS	EPC2::PHF1
20	LG-ESS	JAZF1::SUZ12
21	LG-ESS	JAZF1::PHF1
22	ESS (grade unknown)	
23	ESS (grade unknown)	
24	ESS (grade unknown)	
25	HG-ESS	
26	HG-ESS	YWHAE::NUTM2A/B/E
27	ESN (mixed with leiomyoma)	SF1::CSNK1G1
28	HG-ESS	YWHAE::NUTM2A/B/E
29	ESS (grade unknown)	BCOR ITD
30	ESS (grade unknown)	GLI3::IGFBP1 UBE2E2::SCAP
31	LG-ESS	JAZF1::SUZ12
32	LG-ESS	MEAF6::PHF1
33	ESS (grade unknown)	
34	HG-ESS	CEP128::ADCK1 MIR31HG::SULF1 FGFR3::MAEA
35	HG-ESS	YWHAE::NUTM2A/B/E
36	HG-ESS	CRY2::CCDC73
37	HG-ESS	LPP::TP63 RB1::THSD1
38	LG-ESS	JAZF1::SUZ12
39	LG-ESS	
40	UUS	
41	UUS	PHAF1::NFAT5 MGA::NUTM1
42	UUS	
43	UUS	
44	UUS	AP3B2::CALCOCO1
45	HG-ESS	ZC3H7B::BCOR

(continued in next column)

TABLE 1. Diagnosis and fusion Transcripts Identified in 47 Endometrial Stromal Tumors (continued)

Patient	Diagnosis	Fusion Transcripts
46	ESS (grade unknown)	MIER2::PTPRM
47	LG-ESS	

Abbreviations: ESN, endometrial stromal nodule; HG-ESS, high-grade endometrial stromal sarcoma; ITD, internal tandem duplication; LG-ESS, low-grade endometrial stromal sarcoma; NOS, not otherwise specified; UUS, undifferentiated uterine sarcoma.

^aCase already published in Panagopoulos et al,⁷ Panagopoulos et al,⁶ Micci et al,¹³ and Micci et al.³

cumulative proportion of explained variance larger than 80% were retained for clustering to achieve a dimensional reduction. The sample scores of the selected relevant PCs were clustered by hierarchical clustering²¹ with Euclidean distance and Ward minimum variance linkage.²² A dendrogram resulting from hierarchical clustering was visually inspected to determine the best-suited number of clusters.

Validation of the Top Ten Hypermethylated and Hypomethylated Genes

Several important CpG sites were selected for validation and interpretation. To achieve this, the *Between-Cluster Sum-of-Squares* (BCSS)²³ index was calculated for all CpGs. This index represents the total variation in the sample for a specific CpG, minus the within-subtype variation of that same CpG, summed across the subtypes. For this purpose, only LG-ESS and HG-ESS, as well as UUS, were used because their subtype identification was the most reliable. The 100 CpGs with the largest BCSS index values were used as a reduced selection for better visualization of the clustering results using heatmaps. Additionally, methylation data for CpGs included in the reduced selection that also had a corresponding gene were used to calculate the within-subtype means. The genes associated with the 10 largest (smaller) values of mean within-subtype methylation were further examined and interpreted as highly (lowly) expressed genes.

RNA Sequencing

RNA sequencing was performed on 21 samples (cases 27–47). For this purpose, 200 ng of total RNA was sent to the Genomics Core Facility at the Norwegian Radium Hospital, Oslo University Hospital, for high-throughput paired-end RNA sequencing.¹⁶ The FASTQC software was used for quality control of the raw sequence data (available online at Babraham Bioinformatics).²⁴ Fusion transcripts were identified using FusionCatcher software.^{25,26}

Reverse Transcription Polymerase Chain Reactions and Sanger Sequencing Analyses

The primers used for polymerase chain reaction (PCR) amplification and Sanger sequencing analyses are listed in

Appendix Table A1 and have been reported in previous studies.^{6,7,13,27} Complementary DNA synthesis, reverse transcription PCR amplification, and Sanger sequencing were performed as previously described.¹⁰ Sequencing was conducted using an Applied Biosystems SeqStudio Genetic Analyser System (Thermo Fisher Scientific). The Basic Local Alignment Search Tool (BLAST)²⁸ and BLAST-like alignment tool (BLAT)²⁹ were used for the computer analysis of sequence data.

RESULTS

Methylation Profile

All tumors investigated for methylation status showed informative results. PCA of the gene methylation values for all probes, followed by hierarchical clustering in the reduced PCA space, was used to visualize the differences in DNA methylation for each tumor. Using this approach, we observed that the 24 LG-ESSs were consistently clustered under two main trees (Fig 1). Two main clusters were identified for HG-ESS, while three of the five UUSs were clustered together. Some tumors of different histologies were interspersed, with two HG-ESSs and two USSs clustering among the LG tumors (Fig 1). Consistent with their aggressive nature, USSs were found to cluster closely with HG-ESSs.

When focusing solely on LG-ESS, HG-ESS, and UUS, we identified 76 genes that were differentially methylated across one to three CpG sites based on the BCSS analysis. Among the histologic subtypes, 20 genes in each entity showed a BCSS value between 1.2 and 3.8 (Fig 2) and a unique methylation profile with a unique gene pattern. The *LMX1B* gene (in the *LMX1B-cg04996334* and *LMX1B* CpG sites; BCSS 2.2 and 1.3) and *miR34C* (BCSS 1.2) were found to be methylated in both LG-ESS and HG-ESS. Additionally, *CFAP45* (BCSS 2.4), *HDAC4* (1.9), *ACY3* (1.5), *MOB3A* (1.43), *VPS13B* (1.4), *PHACTR2* (1.37), and *XXYL1* (1.2) were methylated for HG-ESS and UUS, while *miR34B* was methylated (BCSS 1.5) in both LG-ESS and HG-ESS. The highest value was reported for nuclear factor of activated T cytoplasmic 1 (*NFATC1*; LG-ESS; BCSS 3.8), and the lowest value was reported for *miR34C* in LG-ESS and HG-ESS (BCSS 1.2).

Fusion Gene Identification

All tumors sent for transcriptome sequencing provided informative results; however, only 14 samples showed the presence of fusion transcript(s) after analysis using the FusionCatcher algorithm. Six tumors showed the presence of the already known fusion genes: the *JAZF1::SUZ12* and *MEAF6::PHF1* fusions were found in three LG-ESS cases (cases 31 and 38 and case 32, respectively), *YWHAE::NUTM2A/B/E* was found in two HG-ESS cases (cases 28 and 35), and *ZC3H7B::BCOR* was found in case 45. Thirteen new putative fusions were found in eight cases (one to three specific transcript(s) per case). Internal tandem

duplication (ITD) of the *BCOR* gene was noted in case 29. All transcripts, fusions, and ITD were validated by PCR, followed by Sanger sequencing/cycle sequencing. An overview of the fusion and breakpoint positions is presented in Figure 3 and Table 1.

DISCUSSION

Specific chromosomal aberrations have been described in ESS, the most common of which are translocations involving two different chromosomes. Genes altered by chromosomal rearrangements, namely *PHF1*, *JAZF1*, *MEAF6*, *EPC1*, *EPC2*, and *BRD8*, function as transcriptional regulators either through the formation of zinc finger motifs or through epigenetic regulation.⁴ For example, *PHF1* and *SUZ12* are members of the polycomb repressive complex family (mainly the polycomb repressive complex 2 subunits), and *BCOR* is part of the PRC complex that promotes transcriptional repression by the covalent modification of histone deacetylases and the polycomb repressive complex. As various genes altered in ESS play a role in epigenetic regulation, either through polycomb-mediated gene silencing or post-transcriptional covalent modification of histone proteins, we hypothesized that different subgroups in the EST spectrum would have similar methylation profiles, independent of which genes were rearranged. Kommoss et al³⁰ reported specific DNA methylation signatures in a set of uterine neoplasms, including the LG and HG subtypes. They identified distinct methylation clusters between the LG-ESS and HG-ESS, as well as between HG-ESS with *YWHAE::NUTM2* and *BCOR* rearrangements. By and large, our findings on HG-ESS and LG-ESS are similar to those reported by Kommoss et al as these two subgroups clustered separately. Unfortunately, it is not possible to perform any comparison at the gene level as that type of information was only provided in our study. Furthermore, we report here for the first time, to our knowledge, the methylation pattern for USS showing that the profile for this subtype clustered close to that of HG-ESS with *BCOR* rearrangements.

The DNA methylation profile showed that HG-ESS with the *ZC3H7B::BCOR* fusion clustered at one end of the unsupervised analysis, alongside three tumors that were morphologically identified as UUS but for which no fusion was detected. This suggests a shared molecular pathway among these tumors. The LG-ESS clustered together into two subgroups separated by six tumors, five HG-ESSs and 1 UUS.

Among the differentially methylated genes, several showed a specific profile for each subgroup, suggesting that the methylation status is unique in different EST entities with unique gene methylation signatures. A few genes showed a similar methylation pattern in two of the entities, such as *LMX1B* and *miR34C*, which were similarly methylated in both LG-ESS and HG ESS. Additionally, *CFAP45*, *HDAC4*, *ACY3*, *MOB3A*, and *XXYL1* showed comparable methylation in HG-ESS and UUS. The highest methylation value was reported for *NFATC1*, and the lowest was detected for *miR34C* in LG-ESS

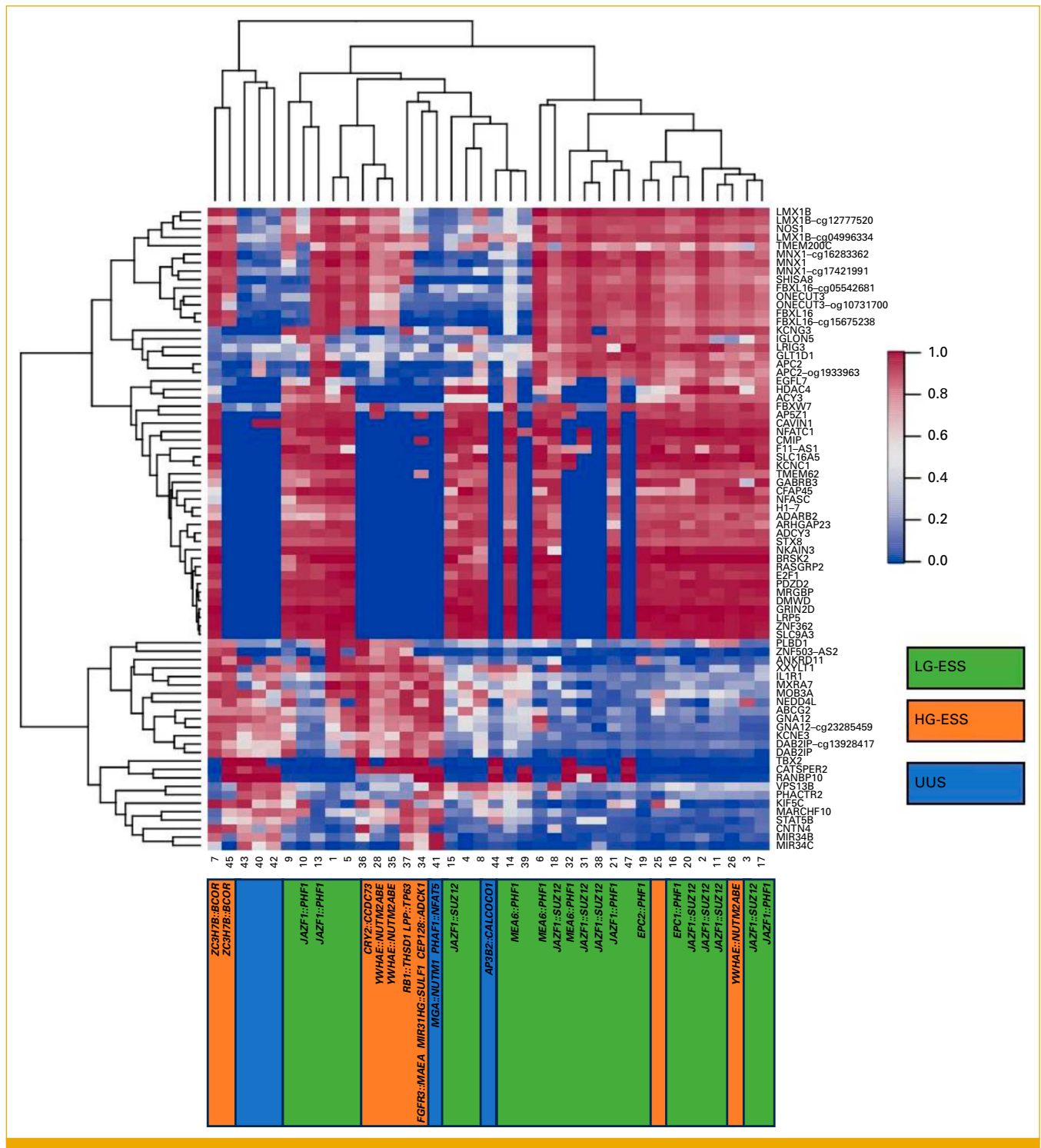


FIG 1. Methylation profile of EST tumors. In green (LG-ESS), in orange (HG-ESS), and in blue (UUS), with the related fusion transcripts identified. EST, endometrial stromal tumor; HG-ESS, high-grade endometrial stromal sarcoma; LG-ESS, low-grade endometrial stromal sarcoma; UUS, undifferentiated uterine sarcoma.

and HG-ESS. The nuclear factor of activated T cytoplasmic 1 (NFATC1) is a transcription factor that has important functions in many tumors.³¹ *miR34c* is a tumor suppressor gene that induces cell apoptosis and inhibits cell proliferation and invasion in various tumor cells.³²

A common theme in ESS is that known fusions are characterized by genomic rearrangements involving two chromosomes, for example, t(7;17) (p15;q21) and t(6;7) (p21;p22). Similarly, we identified two new fusion transcripts in HG-ESS involving genes from chromosomes 8 and 9 (case

3.8

LG-ESS	HG-ESS	UUS
NFATC1	CFAP45	CATSPER2
SLC16A5	LMX1B	RANBP10
KCNC1	HDAC4	AP5Z1
GRIN2D	MNX1	CFAP45
LRP5	MNX1-cg16283362	STX8
ZNF362	SHISA8	H1-7
CMIP	APC2	GABRB3
LMX1B	NEDD4L	ARHGAP23
TBX2	ACY3	ADARB2
FBXW7	EGFL7	HDAC4
DAB2IP	IGLON5	TMEM62
MIR34B	MOB3A	GNA12
ZNF503-AS2	VPS13B	ACY3
KCNE3	APC2-cg19333963	MIR34B
KIF5C	MNX1-cg17421991	STAT5B
STAT5B	PHACTR2	MOB3A
DAB2IP-cg13928417	MXRA7	VPS13B
CNTN4	LMX1B-cg04996334	PHACTR2
LMX1B-cg04996334	XXYL1	MARCHF10
MIR34C	MIR34C	XXYL1

1.2

FIG 2. Differentially methylated genes^a within the histologic subtypes of ESS.

^aGenes with the same methylation pattern are presented in bold; green is used to denote the highest value and red the lowest values.

34), in ESN involving chromosomes 11 and 15 (case 27), in UUS involving chromosomes 12 and 15 (case 34), and in ESS with an uncertain subtype involving chromosomes 18 and 19 (case 46).

In HG-ESS, the long noncoding RNA (lncRNA) *MIR31HG* (mapping on 9p21) is fused with the tumor suppressor sulfatase 1 (*SULF1*; on 8q13). To the best of our knowledge, this is the first time that a lncRNA has been shown to be involved in a fusion. The *MIR31HG* is aberrantly expressed in different solid malignant tumors³³ and affects numerous biological processes during tumorigenesis, including proliferation, metastasis, epithelial-mesenchymal transition, cellular senescence, and apoptosis.³⁴ Its dysregulation in various cancers is significantly related to various stages of disease progression, making it a potential biomarker for diagnosis and prognosis and a promising target for treatment.³⁴

Fusion of splicing factor 1 (*SF1*) and the casein kinase 1 gamma 1 (*CSNK1G1*) was identified for the first time in ESN. *SF1* is a transcription factor, and little is known about the role of individual splicing factors in EST. The casein kinase I isoform gamma 1 (*CSNK1G1*) is an isoform of the casein kinase I gene family that plays a crucial role in various cellular processes, carcinogenesis, and cancer progression.

Targeting CK1 holds great promise as a therapeutic strategy against cancer treatment.³⁵

In a UUS, the Adapter Related Protein Complex 3 Subunit Beta 2 (*AP3B2*; mapping on 15q25) is fused with the 3' gene Calcium-Binding and Coiled-Coil Domain-Containing Protein 1 (*CALCOCO1*; on 12q13). The *CALCOCO1* gene functions as a coactivator for nuclear receptors in combination with other NCOA2-binding proteins, such as *EP300*, *CREBBP*, and *CARM1*³⁶ and the aryl hydrocarbon receptor,³⁷ and it is also involved in the transcriptional activation of target genes in the Wnt/ β -catenin pathway.³⁸ The zinc finger C2H2-type domain was retained in the chimeric transcript. Its interaction with NCOA2-binding proteins highlights the similarities with a previously reported *GREB1::NCOA2* fusion in UUS,³⁹ leading to the hypothesis that alterations in NCOA2-regulatory proteins could be a common theme for UUS.

The *MIER2::PTPRM* was detected in ESS with no defined histotype. Mesoderm Induction Early Response 1, Family Member 2 (*MIER2*) is involved in histone deacetylation; however, the biological characteristics and functions of *MIER2* remain unknown.⁴⁰ The protein Tyrosine Phosphatase Receptor Type M (*PTPRM*) regulates a variety of cellular processes, including cell growth, differentiation, mitotic cycle, and oncogenic transformation, and may have a tumor-

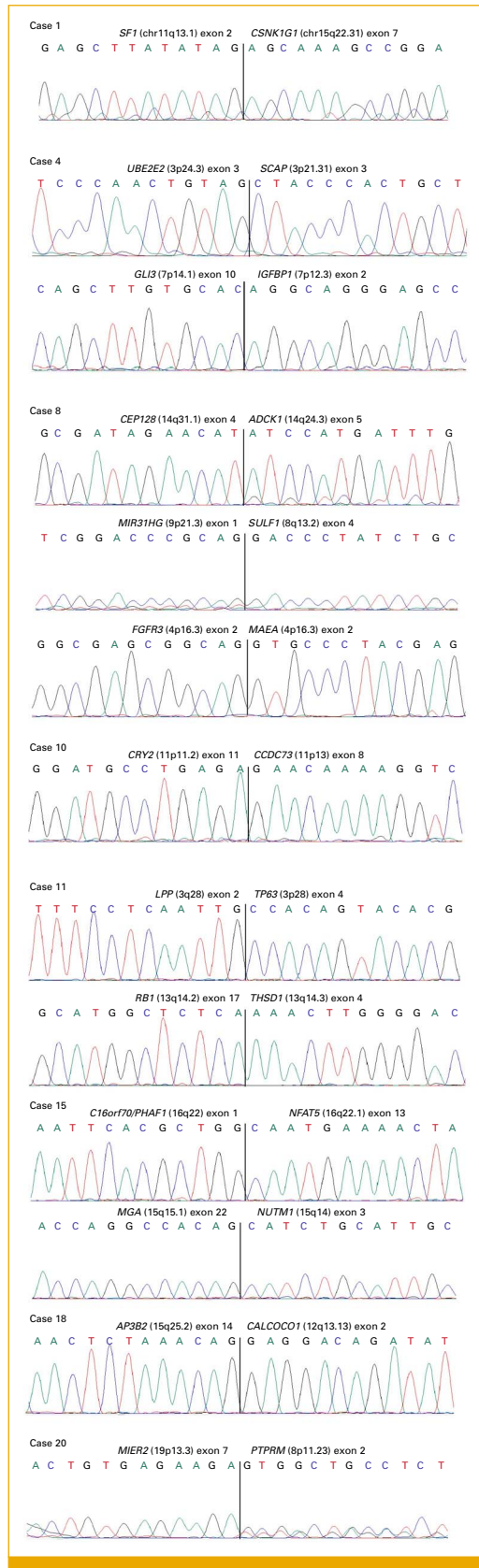


FIG 3. Fusion transcripts validated by PCR. PCR, polymerase chain reaction.

suppressing role; its decreased expression may be correlated with poor prognosis and is inversely correlated with disease-free survival in breast cancer and glioma progression.^{41,42}

Nine additional fusions were identified in this study (see above). Given that the two genes involved in each transcript are mapping on the same chromosomes, a read-through mechanism could be hypothesized to lead to false-positive results. However, validation through PCR and cycle sequencing confirmed their presence as real entities.

The fusion of the GLI Family Zinc Finger 3 (*GLI3*) and the insulin-like growth factor-binding protein 1 (*IGFBP1*) was reported for the first time in ESS with an undefined grade. The transcription factor *GLI3* regulates cell growth by acting as both a tumor initiator and tumor suppressor.⁴³ However, its role in the ESS has not yet been investigated.

In the same tumor, the fusion between Ubiquitin Conjugating Enzyme E2 E2 (*UBE2E2*) and SREBF Chaperone (*SCAP*) has been identified. The *UBE2E2* gene is dysregulated in various types of cancers promoting tumorigenesis and chemotherapy resistance.^{44,45} The chaperone *SCAP* plays an important role in the regulation of lipogenesis and inflammatory responses; however, studies on *SCAP* are limited.⁴⁶

In HG-ESS, we identified the fusion between the Centrosomal Protein 128 (*CEP128*; 14q31) and the aarF domain containing kinase 1 (*ADCK1*; 14q24), and the fibroblast growth factor receptor 3 (*FGFR3*, on 4p16) has been reported in a fusion with the Macrophage-Erythroblast Attacher (*MAEA*; 4p16); both the abovementioned fusion has not been previously reported. The kinase *ADCK1* has been found to be upregulated in colon cancer and promotes tumor formation and metastasis of cancer cells.⁴⁷ *FGFR3* alterations have been shown to contribute to the development and progression of tumors in humans.⁴⁸

In the HG-ESS, we identified, for the first time, a fusion between cryptochrome circadian regulator 2 (*CRY2*) and a coiled-coil domain containing 73 (*CCD73*). *CRY2* genetic dysregulation has been shown to lead to the development of some tumors.⁴⁹ *CCD73* has been previously reported as a driver of different tumors such as squamous cell carcinoma of the lung and adenocarcinoma of the liver.⁵⁰

The Lin-11, Isl-1, and Mec-3 (LIM) domain containing the preferred translocation partner in lipoma (*LPP*, mapping on 3q28) gene was found to be fused with *TP63* in an HG-ESS. Previously, the same fusion was reported in a case of breast adenocarcinoma.⁵¹ *LPP* encodes a member of a subfamily of LIM domain proteins, characterized by an N-terminal proline-rich region and three C-terminal LIM domains. The encoded protein localizes to the cell periphery in focal adhesions and may be involved in cell-cell adhesion and cell

motility. This protein shuttles through the nucleus and may function as a transcriptional coactivator.⁵² More recently, LPP has emerged as a critical inducer of tumor cell migration, invasion, and metastasis.⁵³ Through RNAseq, the 5' *LPP* has been found to be rearranged with *BCOR* in an HG-ESS, however, without the generation of a fusion protein.⁵⁴ The Mitelman database of chromosomal aberrations and gene fusions in cancer⁵¹ reports different partners involved in *TP63* fusions. *TP63* is a member of the p53 family of the transcription factor family.⁵⁵ Fusion genes containing *TP63* have been reported in various hematologic malignancies that convert *TP63* into an oncogene.⁵⁶ Interestingly, the same breakpoint (on exon 4) was observed in one of our transcripts.⁵⁶ The same tumor (case 37; HG-ESS) showed an additional fusion between the retinoblastoma gene (*RB1*) and thrombospondin type 1 domain-containing 1. The chimeric protein predicted from the *RB1::THSD1* fusion contained a truncated linker domain and pocket domain B of *RB1*. The interaction of the *RB1* pocket domains A and B with the linker domain is critical for tumor suppression and E2F regulatory function associated with *RB1*.⁵⁷ Structural rearrangements in *RB1* are exceedingly rare. Exon 17 breakpoints (as in our case) have been reported in multiple tumors, suggesting that this may be a recurrent region for rearrangement.⁵⁸ Whether the active mechanism involves the formation of a chimeric protein or a loss of function in *RB1* requires further investigation.

MGA::NUTM1 was detected in UUS. The predicted chimeric protein retained nearly the entire protein sequence of both

MGA (exons 1–22) and *NUTM1* (exons 3–8). Rearrangement of the *NUTM1* gene characterizes a variety of undifferentiated sarcomas, including spindle cells, round cells, and epithelioid type.^{59–61} In the same tumor, fusion between the nuclear factor of activated T-cell 5, tonicity-responsive (*NFAT5*, mapping on 16q22), and *PHAF1*, to our knowledge, was reported for the first time in this study. *NFAT5* was first identified as a transcriptional regulator of activated T cells,⁶² and the NFAT family is involved in tumor development.⁶³ Members of the NFAT family and their transcriptional regulatory networks regulate multiple processes in tumorigenesis, tumor progression, drug resistance, and chemo/radiotherapy tolerance.⁶⁴ However, the precise functional consequences of the aberration remain unclear in EST.

Although we present the largest series of genomically characterized EST published so far, the size of each subgroup (ESN, LG-ESS, HG-ESS, USS, and the different fusion genes and molecular signatures in each of them) is still too limited to allow statistical correlation with clinical parameters.

In conclusion, the presence of fusion genes is a characteristic of the EST and the genes involved in these chimera function as transcription regulators. The methylation signature seems different for distinct subgroups of the EST spectrum. Furthermore, some genes showed similar methylation levels in different entities, highlighting the presence of a continuum in the tumor profile. Additional studies should investigate the possibility of using the methylation levels of CpG sites at specific gene loci as biomarkers for these tumors.

AFFILIATIONS

¹Section for Cancer Cytogenetics, Institute for Cancer Genetics and Informatics, The Norwegian Radium Hospital, Oslo University Hospital, Oslo, Norway

²Oslo Centre for Biostatistics and Epidemiology, Department of Biostatistics, University of Oslo, Oslo, Norway

³Department of Pathology, The Norwegian Radium Hospital, Oslo University Hospital, Oslo, Norway

⁴Department of Gynaecological Oncology, The Norwegian Radium Hospital, Oslo University Hospital, Oslo, Norway

⁵Department of Pathology, Haukeland University Hospital, Bergen, Norway

⁶Centre for Cancer Biomarkers, Department of Clinical Science, University of Bergen, Bergen, Norway

⁷Department of Gynaecology and Obstetrics, Haukeland University Hospital, Bergen, Norway

CORRESPONDING AUTHOR

Marta Brunetti, PhD; e-mail: brunetti.marta90@gmail.com.

AUTHOR CONTRIBUTIONS

Conception and design: Marta Brunetti, Francesca Micci

Financial support: Francesca Micci

Administrative support: Francesca Micci

Provision of study materials or patients: Marta Brunetti, Anca Mihaela Naas, Ane Gerda Zahl Eriksson, Camilla Krakstad

Collection and assembly of data: All authors

Data analysis and interpretation: Marta Brunetti, Valeria Vitelli, Francesca Micci

Manuscript writing: All authors

Final approval of manuscript: All authors

Accountable for all aspects of the work: All authors

AUTHORS' DISCLOSURES OF POTENTIAL CONFLICTS OF INTEREST

The following represents disclosure information provided by authors of this manuscript. All relationships are considered compensated unless otherwise noted. Relationships are self-held unless noted. I = Immediate Family Member, Inst = My Institution. Relationships may not relate to the subject matter of this manuscript. For more information about ASCO's conflict of interest policy, please refer to www.asco.org/rwc or ascopubs.org/po/author-center.

Open Payments is a public database containing information reported by companies about payments made to US-licensed physicians ([Open Payments](http://OpenPayments.org)).

No potential conflicts of interest were reported.

ACKNOWLEDGMENT

The authors wish to thank Jenny Margrethe Dugstad at the Department of Gynecology and Obstetrics, Haukeland University Hospital, Bergen, Norway, for the excellent technical assistance.

REFERENCES

- Kim K-R, Lax SF, Lazar AJ, et al: WHO Classification of Female Genitale Tumors (ed 5). Lyon, France, International Agency for Research on Cancer, 2020
- Akaev I, Yeoh CC, Rahimi S: Update on endometrial stromal tumours of the uterus. *Diagnostics (Basel)* 11:429, 2021
- Micci F, Gorunova L, Agostini A, et al: Cytogenetic and molecular profile of endometrial stromal sarcoma. *Genes Chromosomes Cancer* 55:834-846, 2016
- Micci F, Heim S, Panagopoulos I: Molecular pathogenesis and prognostication of "low-grade" and "high-grade" endometrial stromal sarcoma. *Genes Chromosomes and Cancer* 60:160-167, 2021
- Nucci MR, Harburger D, Koontz J, et al: Molecular analysis of the JAZF1-JJAZ1 gene fusion by RT-PCR and fluorescence in situ hybridization in endometrial stromal neoplasms. *Am J Surg Pathol* 31:65-70, 2007
- Panagopoulos I, Micci F, Thorsen J, et al: Novel fusion of MYST/Es1-associated factor 6 and PHF1 in endometrial stromal sarcoma. *PLoS One* 7:e39354, 2012
- Panagopoulos I, Thorsen J, Gorunova L, et al: Fusion of the ZC3H7B and BCOR genes in endometrial stromal sarcomas carrying an X;22-translocation. *Genes Chromosomes Cancer* 52:610-618, 2013
- Micci F, Gorunova L, Gatiu S, et al: MEAF6/PHF1 is a recurrent gene fusion in endometrial stromal sarcoma. *Cancer Lett* 347:75-78, 2014
- Micci F, Brunetti M, Dal Cin P, et al: Fusion of the genes BRD8 and PHF1 in endometrial stromal sarcoma. *Genes Chromosomes Cancer* 56:841-845, 2017
- Brunetti M, Gorunova L, Davidson B, et al: Identification of an EPC2-PHF1 fusion transcript in low-grade endometrial stromal sarcoma. *Oncotarget* 9:19203-19208, 2018
- Niu S, Zheng W: Endometrial stromal tumors: Diagnostic updates and challenges. *Semin Diagn Pathol* 39:201-212, 2022
- Mayr D, Horn LC, Hiller GGR, et al: Endometrial and other rare uterine sarcomas: Diagnostic aspects in the context of the 2020 WHO classification [in German]. *Pathologie* 43:183-195, 2022
- Micci F, Panagopoulos I, Bjerkehagen B, et al: Consistent rearrangement of chromosomal band 6p21 with generation of fusion genes JAZF1/PHF1 and EPC1/PHF1 in endometrial stromal sarcoma. *Cancer Res* 66:107-112, 2006
- Reference deleted
- Reference deleted
- Genomics Core Facility. <https://oslo.genomics.no/>
- Aryee MJ, Jaffe AE, Corrada-Bravo H, et al: Minfi: A flexible and comprehensive bioconductor package for the analysis of Infinium DNA methylation microarrays. *Bioinformatics* 30:1363-1369, 2014
- Fortin JP, Triche TJ Jr: Hansen KD: Preprocessing, normalization and integration of the Illumina HumanMethylationEPIC array with minfi. *Bioinformatics* 33:558-560, 2017
- R Core Team: R: A Language and Environment for Statistical Computing. Vienna, Austria. R Foundation for Statistical Computing, 2023
- Johnson RA, Wichern DW: Applied Multivariate Statistical Analysis Applied Multivariate Statistical Analysis (ed 7). Pearson New International Edition; 2014.
- Maimon O, Rokach L: Clustering Methods. Mining and Knowledge Discovery Handbook. Berlin: Springer; 2006:321-352.
- Ward JH Jr: Hierarchical grouping to optimize an objective function. *J Am Stat Assoc* 58:236-244, 1963
- James G, Witten D, Hastie T, et al: An Introduction to Statistical Learning (ed 2). New York, NY, Springer, 2023, pp 604, 13 chapters
- Babraham Bioinformatics. <http://www.bioinformatics.babraham.ac.uk/projects/fastqc/>
- Nicorici D, Şatalan M, Edgren H, et al: FusionCatcher—A tool for finding somatic fusion genes in paired-end RNA-sequencing data. *bioRxiv* 10.1101/011650
- Kangaspekka S, Hultsch S, Edgren H, et al: Reanalysis of RNA-sequencing data reveals several additional fusion genes with multiple isoforms. *PLoS One* 7:e48745, 2012
- Mariño-Enríquez A, Lauria A, Przybyl J, et al: BCOR internal tandem duplication in high-grade uterine sarcomas. *Am J Surg Pathol* 42:335-341, 2018
- BLAST: https://blast.ncbi.nlm.nih.gov/Blast.cgi?PROGRAM=blastn&PAGE_TYPE=BlastSearch&LINK_LOC=blasthome
- BLAT Search Genome. <https://genome-euro.ucsc.edu/cgi-bin/hgBlat>
- Kommoss FK, Stichel D, Schrimpf D, et al: DNA methylation-based profiling of uterine neoplasms: A novel tool to improve gynecologic cancer diagnostics. *J Cancer Res Clin Oncol* 146:97-104, 2020
- Shou J, Jing J, Xie J, et al: Nuclear factor of activated T cells in cancer development and treatment. *Cancer Lett* 361:174-184, 2015
- Yu F, Jiao Y, Zhu Y, et al: MicroRNA 34c gene down-regulation via DNA methylation promotes self-renewal and epithelial-mesenchymal transition in breast tumor-initiating cells. *J Biol Chem* 287: 465-473, 2012
- Tu C, Ren X, He J, et al: The predictive value of lncRNA MIR31HG expression on clinical outcomes in patients with solid malignant tumors. *Cancer Cell Int* 20:115, 2020
- Ruan L, Lei J, Yuan Y, et al: MIR31HG, a potential lncRNA in human cancers and non-cancers. *Front Genet* 14:1145454, 2023
- Long NH, Lee SJ: Targeting casein kinase 1 for cancer therapy: Current strategies and future perspectives. *Front Oncol* 13:1244775, 2023
- Kim JH, Li H, Stallcup MR: CoCoA, a nuclear receptor coactivator which acts through an N-terminal activation domain of p160 coactivators. *Mol Cell* 12:1537-1549, 2003
- Kim JH, Stallcup MR: Role of the coiled-coil coactivator (CoCoA) in aryl hydrocarbon receptor-mediated transcription. *J Biol Chem* 279:49842-49848, 2004
- Yang CK, Kim JH, Li H, et al: Differential use of functional domains by coiled-coil coactivator in its synergistic coactivator function with beta-catenin or GRIPI1. *J Biol Chem* 281:3389-3397, 2006
- Brunetti M, Panagopoulos I, Gorunova L, et al: RNA-sequencing identifies novel GREB1-NCOA2 fusion gene in a uterine sarcoma with the chromosomal translocation t(2;8)(p25;q13). *Genes Chromosomes Cancer* 57:176-181, 2018
- Peng M, Hu Y, Song W, et al: MIER3 suppresses colorectal cancer progression by down-regulating Sp1, inhibiting epithelial-mesenchymal transition. *Sci Rep* 7:11000, 2017
- Sun PH, Ye L, Mason MD, et al: Protein tyrosine phosphatase μ (PTP μ or PTPRM), a negative regulator of proliferation and invasion of breast cancer cells, is associated with disease prognosis. *PLoS One* 7:e50183, 2012
- Burgoyne AM, Palomo JM, Phillips-Mason PJ, et al: PTPmu suppresses glioma cell migration and dispersal. *Neuro Oncol* 11:767-778, 2009
- Matissek SJ, Elsawa SF: GLI3: A mediator of genetic diseases, development and cancer. *Cell Commun Signal* 18:54, 2020
- Zhang RY, Liu ZK, Wei D, et al: UBE2S interacting with TRIM28 in the nucleus accelerates cell cycle by ubiquitination of p27 to promote hepatocellular carcinoma development. *Signal Transduct Target Ther* 6:64, 2021
- Hosseini SM, Okoye I, Chaleshtari MG, et al: E2 ubiquitin-conjugating enzymes in cancer: Implications for immunotherapeutic interventions. *Clin Chim Acta* 498:126-134, 2019
- Lee SH, Lee J-H, Im S-S: The cellular function of SCAP in metabolic signaling. *Exp Mol Med* 52:724-729, 2020
- Ji Y, Liu Y, Sun C, et al: ADCK1 activates the β -catenin/TCF signaling pathway to promote the growth and migration of colon cancer cells. *Cell Death Dis* 12:354, 2021
- Komura K, Hirotsuna K, Tokushige S, et al: The impact of FGFR3 alterations on the tumor microenvironment and the efficacy of immune checkpoint inhibitors in bladder cancer. *Mol Cancer* 22:185, 2023
- Ye Y, Xiang Y, Ozyuc FM, et al: The genomic landscape and pharmacogenomic interactions of clock genes in cancer chronotherapy. *Cell Syst* 6:314-328.e2, 2018
- Gao Q, Liang WW, Foltz SM, et al: Driver fusions and their implications in the development and treatment of human cancers. *Cell Rep* 23:227-238.e3, 2018
- Mitelman F, Johansson B, Mertens F: Mitelman database of chromosome aberrations and gene fusions in cancer, 2025
- Guo B, Sallis RE, Greenall A, et al: The LIM domain protein LPP is a coactivator for the ETS domain transcription factor PEA3. *Mol Cell Biol* 26:4529-4538, 2006
- Ngan E, Kiepas A, Brown CM, et al: Emerging roles for LPP in metastatic cancer progression. *J Cell Commun Signal* 12:143-156, 2018
- Kommoss FK, Chang KT, Stichel D, et al: Endometrial stromal sarcomas with BCOR-rearrangement harbor MDM2 amplifications. *J Pathol Clin Res* 6:178-184, 2020
- Deyoung MP, Ellisen LW: p63 and p73 in human cancer: defining the network. *Oncogene* 26:5169-5183, 2007
- Nagel S, Pommerenke C, Quentmeier H, et al: Genomic aberrations generate fusion gene FOXP2::TP63 and activate NFKB1 in cutaneous T-cell lymphoma. *Biomedicines* 10:2038, 2022
- Harbour JW, Dean DC: The Rb/E2F pathway: Expanding roles and emerging paradigms. *Genes Dev* 14:2393-2409, 2000
- Schieffer KM, Feldman AZ, Kautto EA, et al: Molecular classification of a complex structural rearrangement of the RB1 locus in an infant with sporadic, isolated, intracranial, sellar region retinoblastoma. *Acta Neuropathol Commun* 9:61, 2021
- Diolaiti D, Dela Cruz FS, Gundem G, et al: A recurrent novel MGA-NUTM1 fusion identifies a new subtype of high-grade spindle cell sarcoma. *Cold Spring Harb Mol Case Stud* 4:a003194, 2018

60. Zhu P, Sun K, Lao IW, et al: Expanding the spectrum of NUTM1-rearranged sarcoma: A clinicopathologic and molecular genetic study of 8 cases. *Am J Surg Pathol* 48:930-941, 2024
 61. Arellano Zameza P, Karklins SP, Pena J, et al: High-grade spindle cell sarcoma of the scalp with an MGA::NUTM1 gene fusion in a pediatric patient. *Am J Dermatopathol* 46:101-103, 2024
 62. Lee N, Kim D, Kim WU: Role of NFAT5 in the immune System and pathogenesis of autoimmune diseases. *Front Immunol* 10:270, 2019
 63. Pan MG, Xiong Y, Chen F: NFAT gene family in inflammation and cancer. *Curr Mol Med* 13:543-554, 2013
 64. Lin Y, Song Y, Zhang Y, et al: NFAT signaling dysregulation in cancer: Emerging roles in cancer stem cells. *Biomed Pharmacother* 165:115167, 2023
-

APPENDIX

TABLE A1. Primers used for polymerase chain reactions.

Name	Sequence (5' to 3')	Gene	Accession Number
SF1229FW	CCGCTGGAACCAAGACACAA	<i>SF1</i>	NM_004630.4
CSNK1G1-1475R1	GTGATGGCCGATCCCTATGT	<i>CSNK1G1</i>	NM_022048.5
CSNK1G1-1279R2	CCAGTCGCCGTGACATATCGAA	<i>CSNK1G1</i>	NM_022048.5
GLI3-1656FW	GGAACAGCCCGAAGGAACAA	<i>GLI3</i>	NM_000168.6
IGFBP1-670REV	TGTTGGTGACATGGAGAGCC	<i>IGFBP1</i>	NM_000596.4
UBE2E2E-171FW	TCCACTGAGGCACAAAGAGTTG	<i>UBE2E2E</i>	NM_152653.4
SCAP-800REV	CATGGAAGCGTTCAGTCA	<i>SCAP</i>	NM_012235.4
UBE2E2E-301FW	TATCCAGCAAAACCGCTGCTAA	<i>UBE2E2E</i>	NM_152653.4
SCAP-562REV	CTTGTGCCAGGGAACACTGA	<i>SCAP</i>	NM_012235.4
MIER2-618FW	GGAGATCATGGTGGGACCTC	<i>MIER2</i>	NM_017550.3
PTPRM-691REV	GCATGAAAGAACCTGATGGCA	<i>PTPRM</i>	NM_001105244.2
FGFR3-349FW	CGCCTCCTCGGAGTCCTT	<i>FGFR3</i>	NM_000142.5
MAEA-183REV	CCGCTCAACGTCTTCTCCAG	<i>MAEA</i>	NM_001017405.3
MIR31HG-79FW	GCTGCGACCTGTGCATAACTT	<i>MIR31HG</i>	NR_027054.2
SULF1-629REV	TGCAAAACTGACAAAATGTCT CCG	<i>SULF1</i>	NM_001128205.2
CRY2-1601FW	CCCTTCCTGTGTGGAAGACC	<i>CRY2</i>	NM_021117.5
CCDC73-654REV	TGTTTGATTGTATTGCTTCCCGT	<i>CCDC73</i>	NM_001008391.4
LPP-184FW	AGGCTCAGAGACAGAGCAGAA	<i>LPP</i>	NM_005578.5
TP63-547REV	CTGCGCGTGGTCTGTGTTA	<i>TP63</i>	NM_003722.5
RB1-1725FW	CCCATGGATTCTGAATGTGCTT	<i>RB1</i>	NM_000321.3
THSD1-1368REV	AAGGACATTCCAGGGCAGAC	<i>THSD1</i>	NM_018676.4
MGA-7832FW	CTCCAGAATTAGCAAACAGC AG	<i>MGA</i>	NM_001164273.2
NUTM1-627REV	ACTGAAGGCATGATGGGCTG	<i>NUTM1</i>	NM_001284292.2
PHAF1-186-FW	TTGTCTCCTTAGCTCGGGTC	<i>PHAF1</i>	NM_025187.5
NFAT5-2330REV	TGCTGAGTTGATCCAACAGAC	<i>NFAT5</i>	NM_138714.4
AP3B2-1736 FW	CCAGGATTGCACCTGATGTCT	<i>AP3B2</i>	NM_001278512.2
CALCOCO1-125REV	GTAGGTCCGGGCTACATTGAG	<i>CALCOCO1</i>	NM_020898.3
CEP128- 495FW	GGATACCAAGTCGGAACCTGC	<i>CEP128</i>	NM_152446.5
ADCK1 -659REV	TGCTTCACAGCCAGAACGAG	<i>ADCK1</i>	NM_020421.4